Multi-level-assistance Robotic Platform for Navigation in the Urinary System: Design and Preliminary Tests

M. Finocchiaro[1,3,*], X. T. Ha[2,3,*], J. F. Lazo[4,7,*], C. Lai[4,5,*], S. Ramesh[6,7,*], A. Hernansanz[1], G. Borghesan[2], D. Dall'Alba[6], S. Tognarelli[3], B. Rosa[7], A. Casals[1], N. Padoy[7,8], P. Fiorini[6], J. Dankelman[6], E. Vander Poorten[2], A. Menciassi[3], E. De Momi[4]

[1]*Universitat Politècnica de Catalunya, Spain*, [2]*Katholiek Universiteit Leuven, Belgium*, [3]*Scuola Superiore Sant'Anna, Italy*, [4]*Politecnico di Milano, Italy*, [5]*Delft University of Technology, Netherlands*, [6]*University of Verona, Italy* [7]*ICube, University of Strasbourg, CNRS, France*, [8]*IHU Strasbourg, France*

INTRODUCTION

Ureteroscopy is the gold standard procedure for treatment and diagnosis of upper urinary tract diseases such as carcinoma, urinary strictures and urolithiasis. As a minimally invasive procedure, it implies accessing the organs through natural orifices, avoiding incisions. This is translated in lower risk of infections and shorter recovery time for the patient. However, performing this procedure is a non trivial task and mastering it requires an extensive training. Current challenges related to navigation with traditional instruments inside narrow luminal organs, such as the ureter, could turn into a complex task due to the limited intuitiveness in controlling the endoscope movements, the poor visual feedback, and the absence of any type of guidance or assistance in current endoscopic systems [1].

In this context, Robotic Flexible Ureteroscopy offers an opportunity to overcome the mentioned challenges, ease the burden of the clinicians [2] and offer better treatments for patients. The advantages these robotic systems present include the use of ergonomic Human Machine Interfaces (HMI) which allow more precise and smoother movement of the tools and the possibility to operate the robot remotely at a safer distance from radiation. Nevertheless, since the first reported clinical use of a robotic ureteroscope, the Sensei Magellan system (Hansen Medical, no longer commercially available) [3], few other robotic platforms have been tested for urological applications. This lack of robotic platforms might be related to the fact that the platforms did not provide sufficient assistance to the operator (*e.g.* haptic feedback, augmented reality, autonomous navigation *etc.*), limiting the benefit of their use compared to manual approaches.

In this regard, this abstract introduces the design and a preliminary user test of an innovative robotic platform able to address the current challenges related to navigation in the urinary tract. The proposed platform presents different levels of assistance up to a level 4 of autonomy as defined in [4]. The platform is endowed with (1) a multi-steerable active catheter, (2) multi-level autonomy HMI, (3) a real-time tracking system of the position and shape of the device inside the lumen and (4) real-time suggestions and aids for the user (*e.g.*, current procedure phase, position of the center of the lumen *etc.*). The mechanical properties of the active robotic catheter together with its autonomous and semi-autonomous abilities could help clinicians to prevent perforations and get support during the procedure. Furthermore, thanks to the integrated tracking system, real-time position of the ureteroscope together with its shape mapped inside the patient's anatomy may become available during the whole surgery, reducing the need of using X-rays for localization.

*These authors contributed equally to this work.

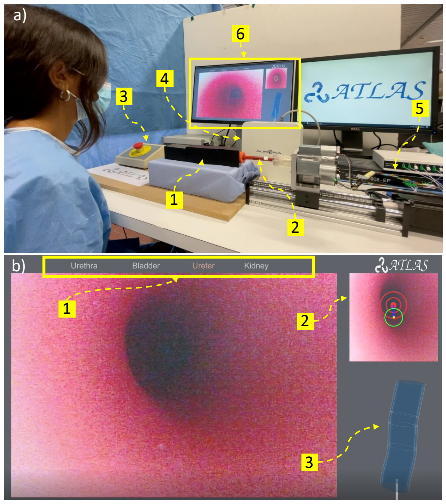

Fig. 1. a) General perspective of the Multi-level-assistance robotic platform including: 1) ureter phantom, presenting the visual conditions of a real ureter; 2) built robotic endoscope; 3) emergency stop button; 4) EM tracking system; 5) FBG interrogator and 6) Human Machine Interface. b) The Graphical User Interface: 1) current phase of the procedure; 2) processed output (center of the ureter) of our visual-servoing module and 3) 3D shape of the endoscope relative to the phantom expressed in the EM coordinate frame.

MATERIALS AND METHODS

The proposed system is depicted in Fig. 1 and it includes three main components:

- A *Visual-Servoing Module*, based on [5], comprises of (1) a cable-driven soft robotic endoscope which has a backbone and a helical structure with two bending directions. The steerable segment of the soft robotic endoscope is 70 mm long which is similar to the one in a ureteroscope; (2) an actuation robotic platform to bend in two directions and to insert the robotic endoscope. In total, there are 3 Degrees of Freedom (DoFs) in Visual-Servoing Module. An Arduino Mega is used to implement two PID controllers and served as a bridge between high-level commands and all the actuators. A deep learning based visual servoing high-level controller is used to autonomously segment the lumen from the camera images, as presented in [6], and compute the center of the ureter. The information from the detected center is used to calculate the error and bring the tip of the endoscope towards the detected center point. The average center detection time is 0.15 s deployed on a NVIDIA GeForce RTX 2080 GPU.

- A *Shape Sensing Module* adapted from [7] includes a multicore Fiber Bragg Grating (FBG) (FBGS, Belgium) embedded in the center channel to sense the 3D shape of the soft robotic endoscope. Two electromagnetic (EM) tracking sensors (NDI, Canada) are attached to the tip and to the base of the robotic scope to localize the 3D reconstructed shape in the EM coordinate frame.
- A multi-level autonomy *HMI* including a Graphical User Interface (GUI) implemented in Unity3D (Unity Technologies, USA) and a joystick for controlling the endoscope in manual or assisted control. The GUI shows: (1) the endoscopic image recorded by the camera, (2) the position and deformation of the endoscope registered in the pre-operative and intra-operative images, (3) the image with higher level features such as computed by the visual-servoing module, and (4) the phase of the procedure.

Three different levels of assistance are considered.

1) *Manual* - The operator can see the endoscopic images recorded by the camera and the information regarding the position and deformation of the endoscope obtained from the shape sensing module. The operator controls the 3 DoFs of the endoscope through a joystick or keyboard.
2) *Visual* assistance - In addition to the information mentioned in the manual scenario, information regarding the detected center of the lumen and the clinical phase is shown to the operator. In this operation mode, the navigation is still performed by the user using the joystick.
3) *Autonomous* - During fully automated intraluminal navigation the visual servoing module drives the endoscope inside the lumen, i.e. the 2 DoF bending and the insertion/retraction, following the center-line detected with the computer vision module. The clinician supervises the procedure and in case there is any concern they can halt immediately the process by pressing the emergency stop button and recover full manual control over the endoscope. In case that the computer vision system fails on detecting the lumen, the robot halts its movement.

As initial test, we performed a set of experiments to compare the capabilities of the system, at its different levels of assistance, for the task of centering the endoscope in the lumen. In the *Manual* and *Visual* scenarios, all participants (10 individuals with non-medical background) allowed to get familiar with the system for five minutes before performing the task in order to exclude possible learning effects. The participants had only one chance and were asked to command the robot, i.e. moving only 2 DoFs for the bending of the tip, to reach the center of the lumen. In the *Autonomous* scenario, the robot performs the task with aid of the visual servoing high-level controller.

The performance metrics taken into account are the settling time and the Steady State Error (SSE). The settling time is defined as the first time the endoscope reaches a distance within less than 20% of the initial distance with respect to the center of the lumen. A condition was herein that this position is maintained for more than one second. The SSE is defined as the distance between the theoretical detected lumen center and the center of the camera frame when the participants or the robot finished the tasks.

RESULTS AND CONCLUSION

A total of 10 participants were considered for the *Manual* and *Visual* feedback experiments. In the case of the *Autonomous* scenario 10 experiments were carried out. Boxplots comparing the results between each of the modalities are shown in Fig. 2.

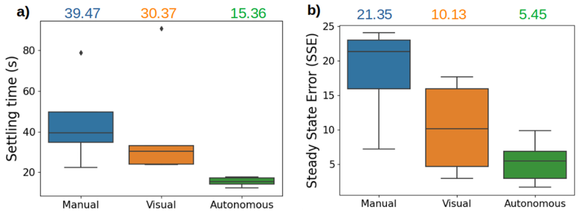

Fig. 2. Boxplots comparison of a) Steady State Error (pixels) and b) settling time between the three modalities of the system (manual control, visual feedback, autonomous) tested for the lumen centering task. The median value for each setting is presented on the top.

In the case of settling time the median values obtained were 39.47, 30.37 and 15.36 s for the manual, visual, and autonomous respectively and the values obtained for SSE were 21.35, 30.37 and 15.36 pixels, respectively. In both metrics the autonomous modality obtains the best performance. In the case of settling time, it reaches the goal in half the time that is required with visual feedback and is 2.5 faster than the case when there is no feedback. For the case of SSE metric the values obtained with visual feedback and manual mode are twice and four times higher than the autonomous mode.

In conclusion, robotic platforms represent an opportunity to reduce the risks and difficulties related to ureteroscopy. This work successfully demonstrated autonomous navigation in a simple ureter phantom using a robotic catheter endowed with real-time shape sensing and localization and a multi-level autonomy HMI. Future work includes (1) integrate FBG/EM trackers data to improve the autonomous control algorithm of the catheter (now used only for shape-sensing and localization), (2) test the whole system in a multi-organ phantom, (3) conduct user tests with expert clinicians.

ACKNOWLEDGEMENT

This work was supported by the ATLAS project. This project has received funding from the European Union's Horizon 2020 research and innovation programme under the Marie Sklodowska-Curie grant agreement No 813782. This work was also partially supported by French State Funds managed by the "Agence Nationale de la Recherche (ANR)" through the "Investissements d'Avenir" (Investments for the Future) Program under Grant ANR-10-IAHU-02 (IHU-Strasbourg).

REFERENCES

[1] V. De Coninck, E. X. Keller, B. Somani, G. Giusti, S. Proietti, M. Rodriguez-Socarras, M. Rodríguez-Monsalve, S. Doizi, E. Ventimiglia, and O. Traxer, "Complications of ureteroscopy: a complete overview," *World journal of urology*, vol. 38, no. 9, 2020.

[2] J. Rassweiler, M. Fiedler, N. Charalampogiannis, A. S. Kabakci, R. Saglam, and J.-T. Klein, "Robot-assisted flexible ureteroscopy: an update," *Urolithiasis*, vol. 46, no. 1, 2018.

[3] M. M. Desai, R. Grover, M. Aron, A. Ganpule, S. S. Joshi, M. R. Desai, and I. S. Gill, "Robotic flexible ureteroscopy for renal calculi: initial clinical experience," *The Journal of Urology*, vol. 186, no. 2, 2011.

[4] A. Attanasio, B. Scaglioni, E. De Momi, P. Fiorini, and P. Valdastri, "Autonomy in surgical robotics," *Annual Review of Control, Robotics, and Autonomous Systems*, vol. 4, pp. 651–679, 2021.

[5] J. F. Lazo, C.-F. Lai, S. Moccia, B. Rosa, M. Catellani, M. de Mathelin, G. Ferrigno, P. Breedveld, J. Dankelman, and E. De Momi, "Autonomous intraluminal navigation of a soft robot using deep-learning-based visual servoing," 2021.

[6] J. F. Lazo, A. Marzullo, S. Moccia, M. Catellani, B. Rosa, M. de Mathelin, and E. De Momi, "Using spatial-temporal ensembles of convolutional neural networks for lumen segmentation in ureteroscopy," *International Journal of Computer Assisted Radiology and Surgery*, 2021.

[7] X. T. Ha, M. Ourak, O. Al-Ahmad, D. Wu, G. Borghesan, A. Menciassi, and E. Vander Poorten, "Robust catheter tracking by fusing electromagnetic tracking, fiber bragg grating and sparse fluoroscopic images," *IEEE Sensors Journal*, vol. 21, no. 20, 2021.